Unit Power Factor Converter to Charge Embarked Supercapacitors

M. Becherif[1,2], M. Y. Ayad[1], A. Henni[3], A. Aboubou[4], M. Wack[1]

[1] SeT Laboratory, UTBM University
Rue Thierry Mieg 90010 Belfort (cedex), France
[2] FC-Lab fuel Cell Laboratory
Rue Thierry Mieg 90010 Belfort (cedex), France
[3] Alstom Power System, Energy Management Business, Alstom France
[4] LMSE Laboratory, Biskra University, 07000, Algeria
phone: :+33 (0)3 84 58 33 46, fax: +33 (0)3 84 58 33 42, e-mail: Mohamed.becherif@utbm.fr

Abstract – **The use of supercapacitors (SCs) in embedded system is quite suitable because of their appropriate characteristics in term of high power capacitance, low serial resistance and their response time. The supercapacitor is a regular capacitor but with the exception that it offers very high capacitance in a small package. Rather than a battery, the supercapacitor energy storage is by means of static charge not by an electro-chemical process. There are three types of electrode materials suitable for the supercapacitor. They are: high surface area activated carbons, metal oxide and conducting polymers. The high surface electrode material, also called Double Layer Capacitor. It stores the energy in the double layer formed near the carbon electrode surface. The electrolyte may be aqueous or organic. The aqueous variety offers low internal resistance but limits the voltage to one volt. In contrast, the organic electrolyte allows 2.5 volts of charge, but the internal resistance is higher. To operate at higher voltages, supercapacitors are connected in series. On a string of more than three capacitors, voltage balancing is required to prevent any cell from reaching over-voltage.**
This paper deals with the conception of an embarked power source using supercapacitors which are charged by means of Unit Power Factor (UPF) electronic converter. These supercapacitors ensure the power supply of an electrical network miniature rail of 150W. The operating principle of this device and some simulation results obtained under Saber software are presented.

I. INTRODUCTION

Until now, the most used direct storage element in electric power supply applications are undoubtedly the accumulators which allow an acceptable autonomy. Their main disadvantage is their low power density. However, the capacitors have high power capability but they can only be considered for applications which require little energy. So, there was thus a relatively lack in terms of storage devices for high power and high energy applications.

With their energetic features situated between those of the batteries and capacitors, the SCs are certainly one of the most suitable electrical engineering components able to fill the deficit of electrical energy storage [1],[2]. Therefore, these new components form an interesting energy storing device filling the gap between the electrolytic capacitors and conventional batteries. So, SCs offer large perspectives for a best management of the embarked electrical energy by the mean of hybridizing different power sources. In such hybrid power source, SCs are used as an auxiliary power unit (APU) added to a main classical source. In this way the resulted power device will be characterized by the association of advantages of two electrical energy features that is to say a high specific energy combined to a high specific power available in a quite long period of time (about some tens to a hundred of seconds). We notice that this association is made possible thanks to power electronic converters [3],[4].

Moreover, this type of power elements combination allows dissociating the mean power sizing from the peak transient power sizing in order to optimize the volume and weight of whole the embarked power system.

In the reference [5] the authors study the association of a photovoltaic generator to SCs in order to ensure the electric train feeding. Two packs of SCs have been used: the first one (SPack2) is outside of the train and it is charged from a second pack (SPack1) under a high current (fast charging). SPack1 is located at the train station where it is charged with a low current (slow charging) from a photovoltaic generator. In this way the train is periodically supplied by an Energy Transferring Mode (ETM: from Pack1 to Pack2).

In this paper we are interesting to add a new low charging mode for the second SCs pack (SPack1) starting from the AC network. Indeed this charger is justified by the fact that the sun is an uncertain energy source. So, when the sky is overcast it is necessary to use another power source that is to say the AC network in order to win a high reliability of the train feeding. We notice that the embarked power supply is constituted with a DC-bus on which the only used power sources (SPack2) and electrical loads are connected by means of power converters. In each train station the SCs are charged through a DC-DC converter connected to a DC link ensured by the domestic one phase's sinusoidal electrical network by means of diodes rectifier and a boost. This double stage converter offers the possibility to charge the SCs in UPF mode.

This UPF charger is especially considered here in the point of view of its sizing process and its control strategy. So, after exposing the proposed power converter and explaining the use control method, some simulations and experimental results are given and compared in a testing and validating process.

II. UPF CHARGER TOPOLOOGY AND SIZING

The load is a miniature train on the scale 1/24th fed by means of SCs (SPack2) which are supplied by the necessary energy at the stopping stations from (SPack1).

The charging of SCs on the quay (SPack1) is carried out double stage AC-DC and DC-DC conversion. The AC-DC converter is based on using controlled rectifier with UPF allowing to absorb a sinusoidal current in phase with the voltage and thus to limit the harmonics creation in the network, see Fig. 1.

The first converter is an AC-DC one combining a diodes double-bridge rectifier and a boost converter. It realises a conversion with sinusoidal absorption and supplies power to the DC voltage stage consisting of the capacitor C. The control technique of this chopper imposes an inductive current having the shape of a rectified sinusoid. Taking into account the voltage variation from the rectifier (from to the maximum value of the network voltage), the chopper must necessarily be a boost one.

The second DC-DC converter is a simple buck converter; it allows controlling the electrical current charging the SCs.

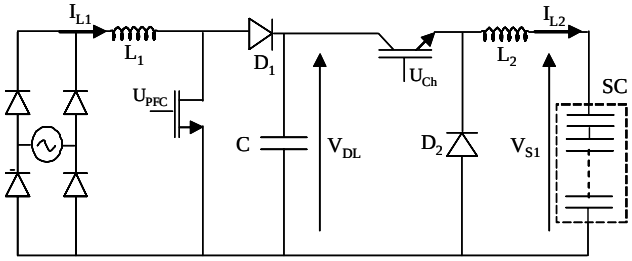

Fig. 1. UPF charger topology

After charging the SCs, the power is provided from these storage elements to the load by using a boost converter (Fig. 2).

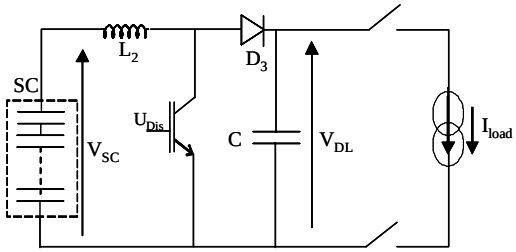

Fig. 2. Discharging SCs to the load

In order to size the above converter we started from the electrical specifications of the miniature train. So, on the base of these specifications one can deduce those of the searched AC-DC-DC converter, see tab 1. In order to be able to reduce the rate of voltage undulation ΔV_{DL}, the capacitor C is placed simultaneously on the continuous part of the rectifier. However, it must be noticed that the AC-DC conversion only through the diode double-bridge inverter has a very power-factor (about 0.6), because of the network current has an impulse form rich in odd harmonics. These impulses quasi centred compared to the sinusoid contribute to deform the sinusoidal waveform of the network voltage by creating a voltage decreases through its internal impedance.

TABLEAU 1

Electrical specifications of the UPF charger

Maximum Power	P_{max} *= 150 W*
Network voltage	V_n = 230 V / 50 Hz
SCs voltage	V_{S1} = 5...10V
Average voltage	$<U_{red}>$ = 10.8V
The voltage factor form	F = 11.1
The rate voltage undulation	**ΔV_C = 48%.**

The proposed solution for this problem is to replace a traditional converter AC-DC by a controlled rectifier with UPF consuming a sinusoidal current in phase with the voltage.

III. EXPERIMETAL BENCH

For the experimental bench (on Fig. 3), we have chosen the SKM 214 A power MOSFET module with SKHI 21 A/B driver. For the rectifier, we will use the GBPC-35A diode module. By using these elements, we find the efficiency of the system is equal to 83% (27% of losses including commutation and conduction MOSFET losses, commutation and conduction MOSFET losses, and inductance losses).

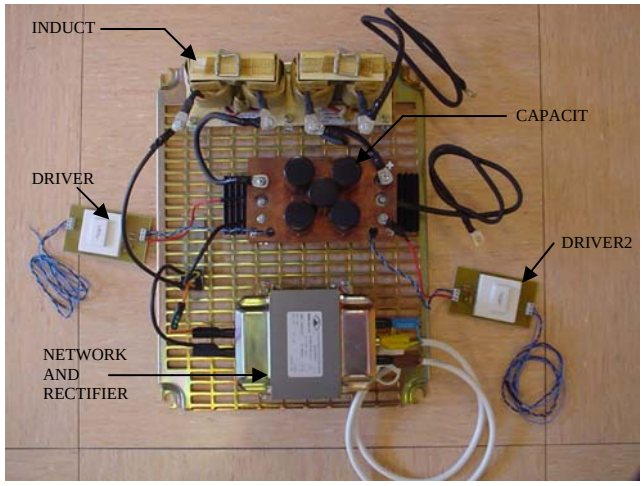

Fig. 3. Realised system

III. STATE SPACE MODELLING

This section gives the dynamic model of the system of Fig. 1. It is composed of a charging machine, a diodes-bridge converter, a Boost converter, a DC Bus, a Buck converter and a Supercapacitor.

The design of the wind generator as well as the storage device using supercapacitors was explained in [7].

The wind generator is composed by a mechanical propeller and a Permanent Magnet Synchronous Machine (PMSM) giving a rated electric power of 150W. The PMSM is driven under a variable speed (situated between 27rd/s and 78rd/s on the basis of the wind profile of Wide hen-Nord Pas de Calais-France).

The PMSM is a single phase machine for which the equivalent electrical scheme is given by the Fig. 4.

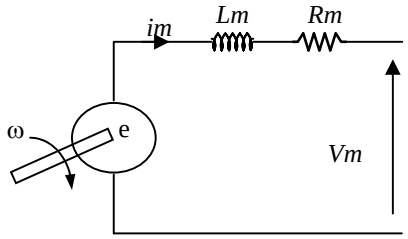

Fig 4. Single phase machine model

The machine parameters are:

$R_m = 0.14\Omega$; $L_m = 0.22mH$; $p = 2$; $\Phi_{\max} = 0.19Wb$

The electromagnetic torque is given by $T_e = p\phi_f i_m$

Where ϕ_f is the machine magnetic flux, p is the poles pair number and i_m is the stator current.

According to Fig. 1, the machine inductance L_m can be considered in serial with the Boost inductance L_1, and then an equivalent inductance is adopted

$$L_{eq} = L_1 + L_m \tag{1}$$

The machine state space is

$$\frac{di_m}{dt} = \frac{1}{L_m}\left[e - V_m - R_m i_m\right] \tag{2}$$

The current and voltage after the diode bridge are:

$i_d = |i_m|$; $U_d = V_m Sign(i_m)$

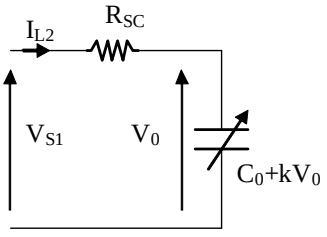

Fig. 5 Supercapacitor electrical model

The DC bus is modeled by:

$$\frac{dV_{DL}}{dt} = \frac{1}{C} i_{DL} = \frac{1}{C}\left[U_{PFC} i_{L1} - U_{Ch} i_{L2}\right] \tag{3}$$

For the Buck converter he model is (see Fig. 5):

$$\frac{di_{L2}}{dt} = \frac{1}{L_2}\left[U_{Ch} V_{DL} - R_{SC} i_{L2} - V_0\right] \tag{4}$$

Finally, the SC is modeled by:

$$\frac{dV_0}{dt} = \frac{1}{C_0 + kV_0} i_{L2} \tag{5}$$

Where $C_0 + kV_0 > 0$

The system can be modeled by a state space approach using the following state space vector:

$$x = \left[x_1;\ \ x_2;\ \ x_3;\ \ x_4\right]^T = \left[i_m;\ \ V_{DL};\ \ i_{L2};\ \ V_0\right]^T \tag{6}$$

The control vector is:

$$u = \left[U_1;\ \ U_1\right]^T = \left[U_{PFC};\ \ U_{Ch}\right]^T \tag{7}$$

Note that $U_2 = U_{Ch} = U_{Dis}$, the subscript *Ch* indicates the charge mode and *Dis* the discharge one.

The dynamic of the system is:

$$\begin{aligned}
\dot{x}_1 &= \frac{1}{L_{eq}}\left[e - R_m x_1 - U_1 x_2 \sigma\right] \\
\dot{x}_2 &= \frac{1}{C}\left[U_1 x_1 \sigma - U_2 x_3\right] \\
\dot{x}_3 &= \frac{1}{L_2}\left[U_2 x_2 - R_{SC} x_3 - x_4\right] \\
\dot{x}_4 &= \frac{x_3}{C_0 + kx_4}
\end{aligned} \tag{8}$$

With $\sigma = 1$ if $i_m \geq 0$ else $\sigma = -1$, $C_0 + kx_4 > 0$

IV. CONTROL STRATEGY OF THE CHARGER

In this section we give some details about the control strategy of both the converter stage i.e. AC-DC (double bridge rectifier combined to the boost chopper) and DC-DC (buck chopper) stage.

A. Regulation of boost charger converter

The boost regulation is of type of power-factor correction. It makes it possible to have a current in phase with the voltage in the chopper input.

The Fig. 6 shows, the control scheme of the boost converter in which the measured voltage V_{DL} is multiplied by the ratio of the maximum current value to the maximum voltage value; the output magnitude is then compared with the measured current value of the boost converter (flowing the inductor L_1). The result of this hysteretic comparison is used to control the converter.

This regulation permits to have a current in phase with the voltage, which reduce pollution in harmonic on the network. However, by using this type of regulation, we do not choose the duty cycle, neither the chopping frequency of the converter. Hence, it should be made sure that the converter supports the frequencies imposed by this control, and to take into account in the inductance sizing.

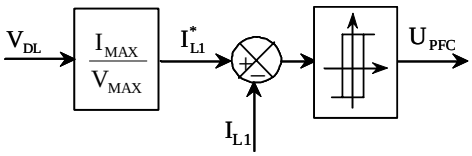

Fig. 6: Control of the boost converter

The current gain I_{MAX} allows regulating the charging current value of the SC to the reference. The voltage gain V_{MAX} allows to be brought back to a sinusoid whose amplitude is only defined by the current gain I_{MAX}.

The effective voltage of the rectifier is equal to 17V; we obtain the value of the gain voltage V_{MAX} equal to 0.023 V.

In order to regulate the commutation frequency of the converter, we use a controlled PWM as for example the one resulting from the comparison of a duty cycle with a serrated signal.

B. Regulation of the SCs buck converter

The Fig. 7 shows the control scheme of SCs charging. First of all, the voltage value of the DC stage must be of 15±0.5V; a hysteretic regulator has been used to verify this condition.

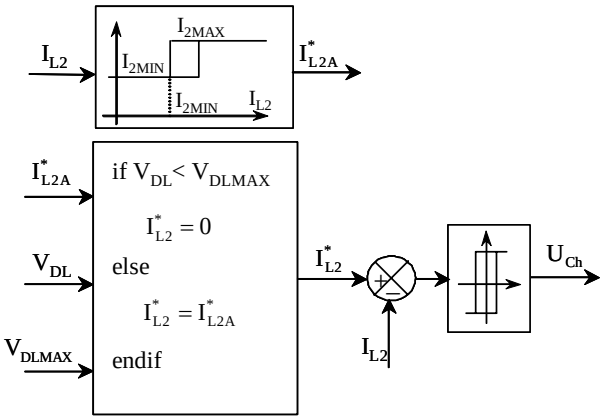

Fig. 7: Control of the SCs converter

with: I_{2MIN}=22 A and I_{2MAX}=23 A.

Then, the SCs are charged under a constant current (22.5A) ensured also by a hysteresis regulator with 1A of bandwidth.

C. Control of the end of charge

In order to stop the charge of the SCs when its voltage reached 10V, we added a condition on the control of the SCs voltage. The SC current reference is equal to zero when the SC voltage is greater than V_{SCmax}.

D. Regulation of the SCs discharging

The Fig. 8 chows the control scheme of SCs discharging. From the power needed by the load and dividing by the SCs voltage, the discharging SCs reference is generated.

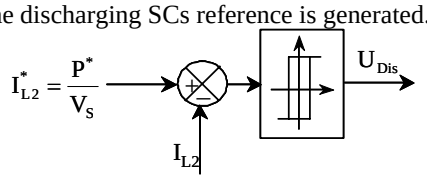

Fig. 8: Control of the SCs discharging

V. SIMULATION RESULTS

The simulations have been achieved by using the Saber software. In this section we present the simulation results highlighting the different functionalities of the studied converter. We are interested in the current and voltage waveforms in the most important points of the converter.

The Fig. 9 proofs that the proposed converter really absorbs a sinusoidal current from the AC network.

However, we see a great peak of this current in the beginning of the converter operating. This phenomenon is certainly due to considering a perfect voltage source, i.e. without internal impedance, but also because of the capacitors filter.

Hence, an inductance of 0.1 mH has been added, between the rectifying bridge and the source, in order to decrease the current.

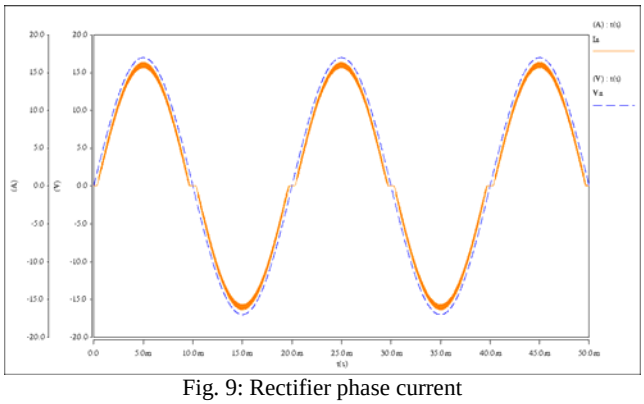

Fig. 9: Rectifier phase current

Figures 10 and 11 present respectively the input current of the boost and its reference ($I^*_{L1} = I_{L1ref}$ and I_{L1}).

Fig. 12 shows the waveforms of the SCs current I_{L2} and voltage v_{s1}. One can notice the existence of hysteric bandwidth of current; by examining its zoom, one may clearly see that this current vary between 22V and 23V. In the same time the DC link voltage V_{s1} is varying also within a voltage hysteretic bandwidth equals to 1 V around 15V. Indeed, this value of DC link voltage is the guarantee of the SCs charging until 10V. For that reason we chose to start the SCs charging only when the DC stage voltage reaches 15V±0.5V. So, the final value of the duty cycle of the buck chopper is about 0.66.

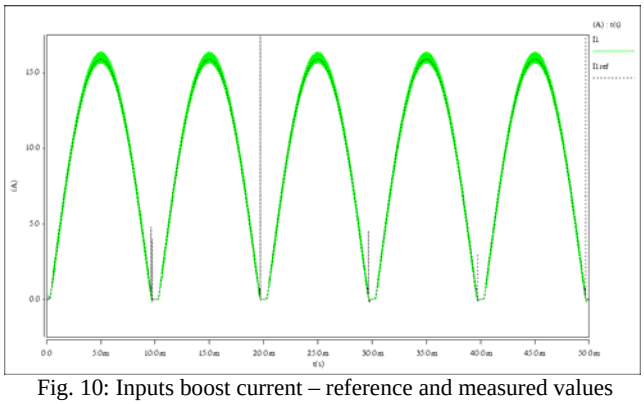

Fig. 10: Inputs boost current – reference and measured values

The waveforms presented in the Fig. 13 correspond respectively to the SC converter control the detection of the charging authorization, the SCs current, the DC link voltage and the SCs voltage (redundancy with Fig. 14).

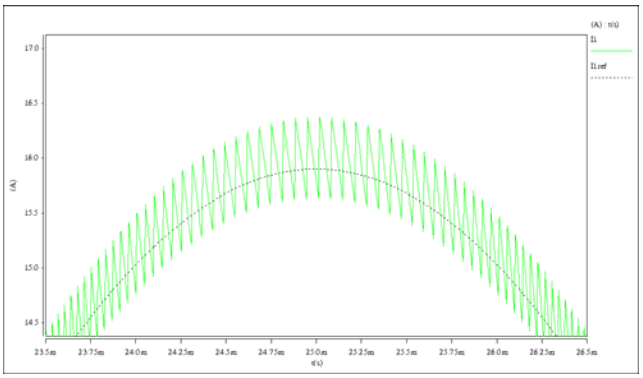

Fig. 11: DC link current wave form

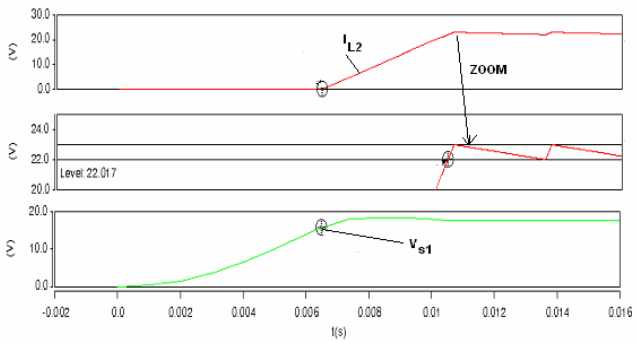

Fig. 12:. SCs current and voltage

From 0ms to 8ms, corresponds to the load of the capacitors situated between the two choppers. From 8ms to 37ms, the chopper series charges the supercondensateurs with constant current. At the end, the capacitor voltage on the DC link decrease to 14.25 V. It is necessary thus to wait the end of this part, that this voltage reached 15.75 V to start to SCs charging. From 56ms to 62ms, we start to charge the SCs, but because the capacitors voltage which decreases again to 14.24 V, the set point of the charging current was not reached.

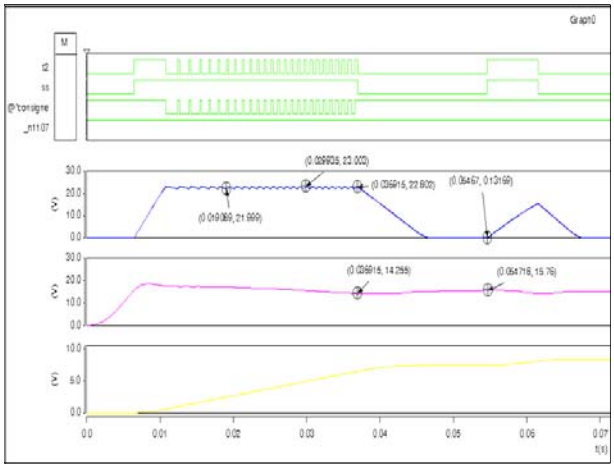

Fig.13: Control of the SC converter, charging authorization, SCs current, condition on the charging SCs voltage, SCs current, DC link voltage and the SCs voltage

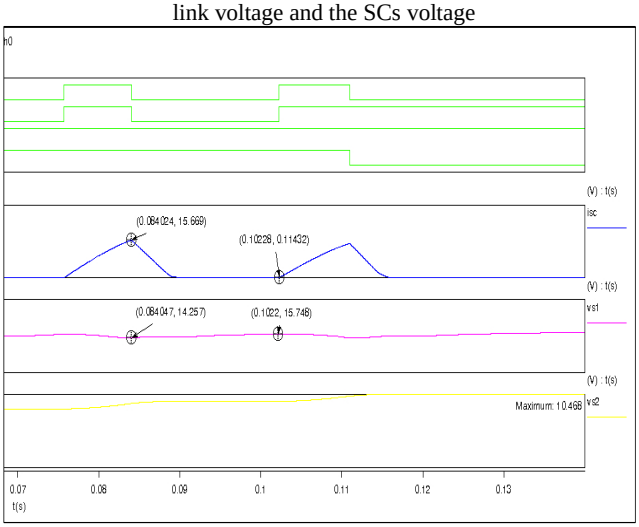

Fig.14: Control of the SC converter, charging authorization, SCs current, condition on the charging SCs voltage, SCs current, DC link voltage and the SCs voltage

From 56ms to 62ms, we continue the charging of the SCs until we obtain the limiting voltage value of 10 V.

VI. VALIDATION EXPERIMENTAL TEST BENCH

In order to test the proposed control strategy of the system shown in Fig. 1, an experimental test bench has been made. This bench is based on the studied device. The wind generator is replaced with the single phase AC network through a transformer. The rest of the circuit has been build

according to the real characteristics described below. On Fig. 15 the different components of the bench are shown. For the control strategy implementation, the dSpace real time interface (RTI) DS1104 has been used. For conditioning the measurement and the control signals between the RTI and the power sides of the system, an electronic card has been developed.

Fig. 16 (top) shows the experimental waveforms of the boost current following well its reference varying as the absolute value of a sine function. The presence of some current delay in the tracking is caused by the delay in the data acquisition and control devices. The simulation waveforms of the figure 10 are then validated. The input AC voltage time variation and the command signal of the boost switch are presented in Fig. 16 (bottom). These results prove that the device sizing and the control strategy are satisfactory. Thus, it can be concluded that the charger is now ready to be explored in order to check the device performances.

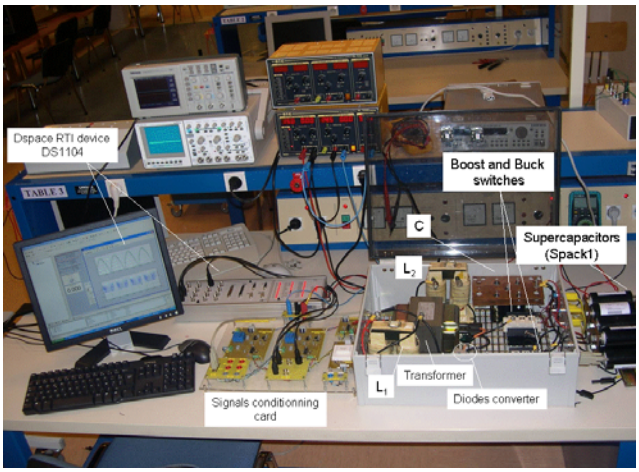

Fig. 15: Experimental Set-up.

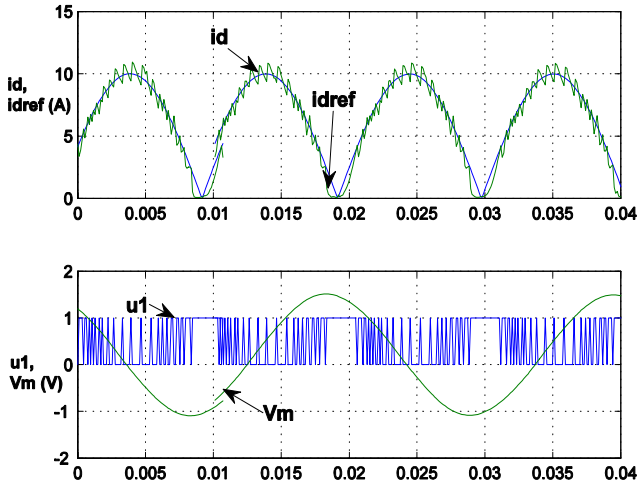

Fig. 16: Experimental Waveforms for currents, control and voltage (V_m/10).

VII. CONCLUSION

In this article, a supercapacitors charger with unit factor power was presented. The design and the sizing were discussed. The control of this system was developed to achieve an unitary power factor.

The state space modelling of the whole system is given.

Some simulation, by using SABER environment, was presented. These results give the good functioning and the experimentations validate the proposed schemes, sizing and control strategies.

VIII. REFERENCES

[1] F. Belhachemi, S. Raël, B. Davat, "A Physical based model of power electric double-layer supercapacitors", IEEE-IAS'00, Rome, October 2000

[2] B.E. Conway, "Electrochemical supercapacitors – Scientific fundamentals and technological applications", Kluwer Academic/Plenum Publishers, New York, 1999.

[3] A. Rufer, "A Supercapacitors-Based Energy-Storage System for Elevators with Soft Commutated Interface", IEEE transactions on industry applications, vol. 38, pp. 1151-1159September/October 2002.

[4] M. Y. Ayad, S. Raël, S. Pierfederici, B. Davat "Supercapacitors for embarked systems as a storage energy device solution " in *Proc. ESSCAP 2004 (CDROM' 171),*, BELFORT, Novembre 2004.

[5] M. Becherif and E. Mendes, "Stability and robustness of Disturbed-Port Controlled Hamiltonian system with Dissipation", 16th IFAC World Congress, Prague, 2005.

[6] M. Becherif, R. Ortega, E. Mendes and S. Lee, "Passivity-based control of a doubly-fed induction generator interconnected with an induction motor", 42nd Conf. on Decision and Contr., pp.5657-5662, Maui, Hawai USA 2003.

[7] M. Becherif, M.Y. Ayad, A. Djerdir and A. Miraoui, "Electrical train feeding by association of supercapacitors, photovoltaic and wind generators", IEEE-ICCEP, 2007.

[8] M. Becherif, M.Y. Ayad and A. Miraoui, "Modelling and passivity-based control of hybrid sources: Fuel cell and supercapacitors". *In* 41st IEEE-IAS, USA, 2006.

[9] M. Y. Ayad, M. Becherif, A. Djerdir and A. Miraoui, "Sliding Mode Control of DC Bus Voltage of a Hybrid Sources using Fuel Cell and Supercapacitors for Traction System", International Symposium on Industrial Electronics (IEEE-ISIE'07), Spain 2007.

[10] A. Henni and H. Siguerdidjane, "Robust nonlinear control of a magnetic suspension system". IEEE CCA 2003, pp: 1307- 1312 vol.2

[11] S. Poullain, F. Heliodore, A. Henni, J.L. Thomas and E. Courbon, "Modelling of the dynamic characteristics of the DC line for VSC transmission scheme". Seventh International Conference on AC-DC Power Transmission, pp: 305- 310. 2001.